

LATTICE QCD WITH LIGHT TWISTED QUARKS: FIRST RESULTS

A. SHINDLER

*John von Neumann-Institut für Computing NIC, Platanenallee 6, D-15738 Zeuthen, Germany
E-mail: andrea.shindler@desy.de*

ON BEHALF OF THE EUROPEAN TWISTED MASS COLLABORATION (ETMC)

I report on first results of the ETMC obtained simulating lattice QCD with two degenerate flavours of Wilson twisted mass fermions, for which physical observables are automatically $O(a)$ improved. Recent improvements of the HMC algorithm allow simulations of pseudoscalar masses below 300 MeV on volumes $L^3 \cdot 2L$ with $L > 2$ fm and at values of the lattice spacing $a \lesssim 0.1$ fm.

Keywords: Lattice QCD; Hybrid Montecarlo; Chiral perturbation theory.

1. Lattice QCD

Simulations of lattice QCD are exact on the given lattice up to statistical errors, but many systematic uncertainties have to be controlled to have a reliable comparison between lattice QCD computations and experimental measurements.

- Renormalization and lattice artefacts: the choice of the lattice QCD action enters in the regularization of the theory. For this reason it is important to choose a lattice action that enjoys simple renormalization properties and good scaling behaviour.
- Light quark masses: it is crucial to use algorithms that allow simulations at light enough quark masses in order to eventually bridge the remaining gap between the simulation and the physical points, using chiral perturbation theory¹ (χ PT).
- Finite size effects: the volume has to be large enough in order to avoid systematic uncertainties stemming from the finite size of the system that is simulated.

The final goal is to simulate two light quarks and two non-degenerate heavier quarks keeping under control all these systematic uncertainties. Here I summarize first results for two light flavours obtained using a theoretically well founded lattice QCD action and a highly improved algorithm.

2. Wilson twisted mass QCD

The lattice QCD action has a gauge S_G and a fermionic S_F part. The so called Wilson twisted mass (Wtm) action² is

$$S_F = a^4 \sum_x \{ \bar{\chi}(x) [D_W + i\mu\gamma_5\tau^3] \chi(x) \}, \quad (1)$$

where

$$D_W = \frac{1}{2} [\gamma_\mu (\nabla_\mu + \nabla_\mu^*) - a \nabla_\mu^* \nabla_\mu] + m_0 \quad (2)$$

is the Wilson-Dirac operator, m_0 is the untwisted (bare) quark mass, μ the (bare) twisted quark mass and τ_3 the third Pauli matrix acting in flavour space. While parity-isospin is violated only at $O(a^2)$, the Wtm action has several main advantages:

- The twisted mass provides a sharp infrared cutoff for low eigenvalues².
- Automatic $O(a)$ improvement when m_0 is properly tuned³.
- The renormalization pattern is in many cases greatly simplified^{4,5}.

Note that also with the standard Wilson ($\mu = 0$) formulation $O(a)$ improvement can be obtained, but a whole set of parameters needs to be tuned to achieve this, while with Wtm only one parameter needs to be tuned, m_0 . To be more specific automatic $O(a)$ improvement is at work if the value of m_0 is tuned to be the critical mass m_c . In all the

results presented here the critical mass is obtained tuning the PCAC mass to zero and the role of the quark mass is played by the twisted mass μ . For recent summaries on Wtm see the reviews [6, 7] and references therein.

2.1. Pseudoscalar decay constant

The pseudoscalar decay constant f_{PS} is an important quantity to compute for phenomenological applications (e.g. for the extraction of V_{us} from the ratio f_K/f_π), and can be used to fix the lattice spacing in physical units. With Wtm this computation presents a set of advantages: no improvement coefficients are needed (namely c_{sw} and c_A) due to automatic $\mathcal{O}(a)$ improvement and moreover no renormalization factors (Z_A) are needed². All the uncertainties related to the estimates of these parameters are simply absent. f_{PS} and many other physical quantities have been studied⁸ in the quenched model confirming that automatic $\mathcal{O}(a)$ improvement is at work and that the $\mathcal{O}(a^2)$ effects are small.

3. Algorithms and phase structure

To perform simulations at light quark masses with dynamical fermions, a substantial amount of computer resources is required. At the Lattice 2001 conference the situation was rather dramatic⁹. The low values of the quark masses, the large volume and the small lattice spacing reached in our work became possible only due to recent algorithmic developments^{10,11}. In particular, for all the $N_f = 2$ results reported here we have used our variant of the HMC algorithm described in Ref. [11]. In continuum QCD with $N_f > 1$ chiral symmetry is spontaneously broken at zero quark mass. The order parameter of this phase transition is the chiral condensate that is discontinuous around the massless point. On the lattice Wilson-like actions break explicitly chiral symmetry even in the massless limit. It is then a natural question, if

one is interested in simulations of light quark masses, to understand the chiral phase structure with Wilson-like quarks. Our collaboration has shown in a set of publications^{12,13,14} that there is a non-trivial phase structure at finite lattice spacing with a first order phase transition close to the chiral limit. These results are in agreement with one of the possible scenarios predicted^{15,16} by lattice- χ PT. In this scenario the first order phase transition line extends in the twisted axis direction until a value of the twisted mass $\bar{\mu}$ of order a^2 . As a consequence there is a minimal value of the quark mass that can be simulated at fixed lattice spacing. Both the occurrence of this scenario and the precise value of $\bar{\mu}$ depend on the details of the lattice action, in particular on the choice of the gauge action S_G . The gauge actions so far studied by our collaboration can be parameterized by

$$S_G = \beta \left[b_0 \sum_{x; \mu < \nu} \left(1 - \frac{1}{3} P^{1 \times 1}(x; \mu, \nu) \right) + b_1 \left(1 - \frac{1}{3} P^{1 \times 2}(x; \mu, \nu) \right) \right] \quad (3)$$

with the normalization condition $b_0 = 1 - 8b_1$. $P^{1 \times 1}$ indicates the standard plaquette and $P^{1 \times 2}$ a planar 1×2 rectangular loop. In particular it has been shown¹⁷ that the value of $\bar{\mu}$ decreases if b_1 is properly chosen. The choice of our collaboration was then to use $b_1 = -1/12$ which corresponds to the so called tree-level Symanzik (tlSym) improved gauge action¹⁸. This choice compromises between a smaller value for $\bar{\mu}$ than obtained with $b_1 = 0$ and avoiding problems with big scaling violation possibly induced by a too large value of $|b_1|$.

4. First results

4.1. Setting the scale

In order to compare results obtained at different lattice spacings and to translate the simulations results in physical units, it is necessary to set the scale, i.e. to give the lattice spacing in physical units. Many choices are

Table 1. The parameters for the simulation. In order to convert to physical units, I take the value of r_0/a as computed at the minimal values of the twisted mass simulated, that can be read from Table 2.

β	$L^3 \times T$	$r_0/a(a\mu_{\min})$	a [fm]
3.9	$24^3 \times 48$	5.184(41)	$\simeq 0.096$
4.05	$32^3 \times 64$	6.525(101)	$\simeq 0.075$

Table 2. Current status of the simulations at $\beta = 3.9$ and $\beta = 4.05$ using the parameters in Table 1: current estimates of the pseudoscalar and the renormalized quark masses, the number of trajectories generated after 1500 trajectories of thermalization.

β	μ_R [MeV]	m_{PS} [MeV]	N_{traj}
3.9	$\simeq 18$	$\simeq 270$	5000
	$\simeq 29$	$\simeq 350$	5000
	$\simeq 38$	$\simeq 400$	5000
	$\simeq 45$	$\simeq 430$	5000
	$\simeq 67$	$\simeq 530$	5000
4.05	$\simeq 18$	$\simeq 270$	4200
	$\simeq 34$	$\simeq 370$	3000

possible and some of them are under investigation by our collaboration. Here I present results obtained by using as an hadronic input the force between two static quarks at a certain intermediate distance r_0 ¹⁹. While this quantity can be measured on the lattice very precisely, it has a rather uncertain phenomenological value. Nevertheless it can certainly be used to compare simulations at different lattice spacings. In this proceeding contribution to translate our results in physical units I use the value $r_0 = 0.5$ fm.

4.2. Pseudoscalar mass and decay constant

The current status of our simulations are summarised in Tables 1 and 2. In Table 1 the parameters of our simulations are provided, and in Table 2 current estimates of the pseudoscalar mass m_{PS} and the renormalized quark mass in physical units are given. A rough estimate of the missing renormalization factor can be obtained from our data, using as inputs the available lattice estimates for the strange quark mass and $m_s/m_{u,d} \simeq 26$. In Figure 1 the quark mass dependence of the pseudoscalar mass squared

is shown. The dependence is to a good approximation linear, and the results at different lattice spacings do not show appreciable cutoff effects. I recall that the twisted quark mass in this plot still needs to be renormalized. In Figure 2 I show the dependence

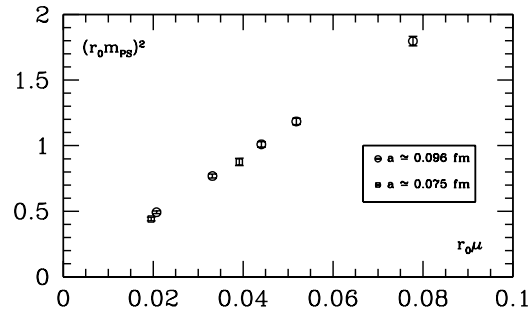


Fig. 1. Quark mass dependence of the pseudoscalar mass squared.

of the pseudoscalar decay constant on the squared pseudoscalar mass. The rather consistent values obtained at the two different lattice spacings is a very promising feature as far as the control on the systematic uncertainties of this physical quantity is concerned. For both the plots I have used χ PT in order to correct for finite size effects²⁰. In a forthcoming publication²¹ we will analyze these data according to χ PT. Here in Fig. 2 I simply show for illustration a linear fit to the 5 lightest pseudoscalar masses, and the phenomenological estimate^{1,22} of the pseudoscalar decay constant in the chiral limit.

5. Conclusions and outlooks

The control of systematic uncertainties on lattice computations is a prerequisite in order to compare them with experimental measurements. I have summarized here some properties of Wtm, together with some first results with $N_f = 2$ light dynamical quarks. These results (see also the proceedings²³ at the Lattice 2006 conference) are rather encouraging and suggest that the systematic uncertainties can be controlled simulating improved lattice actions, with the newly de-

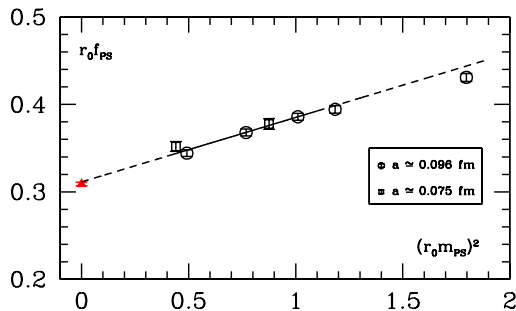


Fig. 2. Dependence of the pseudoscalar decay constant on the squared pseudoscalar mass for 2 different lattice spacings. As a comparison is also shown the phenomenological value (\blacktriangle) in the chiral limit, and a linear fit to the 5 lightest pseudoscalar masses.

veloped algorithms on currently available supercomputers.

Acknowledgments

It is a pleasure to acknowledge all the members of the ETM Collaboration that have contributed to the results presented here. I thank NIC and the computer centres at Forschungszentrum Jülich and Zeuthen for providing the necessary technical help and computer resources. Computer time on UKQCD's QCDOC in Edinburgh²⁴ using the Chroma code²⁵ and on apeNEXT²⁶ in Rome and Zeuthen and on MareNostrum in Barcelona (www.bsc.es) are gratefully acknowledged. This work has been supported in part by the DFG Sonderforschungsbereich/Transregio SFB/TR9-03 and the EU Integrated Infrastructure Initiative Hadron Physics (I3HP) under contract RII3-CT-2004-506078. I also thank the DEISA Consortium (co-funded by the EU, FP6 project 508830), for support within the DEISA Extreme Computing Initiative (www.deisa.org).

References

- J. Gasser and H. Leutwyler *Ann. Phys.* **158** (1984) 142.
- ALPHA** Collaboration, R. Frezzotti, P. A. Grassi, S. Sint, and P. Weisz *JHEP* **08** (2001) 058, [[hep-lat/0101001](#)].
- R. Frezzotti and G. C. Rossi *JHEP* **08** (2004) 007, [[hep-lat/0306014](#)].
- R. Frezzotti and G. C. Rossi *JHEP* **10** (2004) 070, [[hep-lat/0407002](#)].
- C. Pena, S. Sint, and A. Vladikas *JHEP* **09** (2004) 069, [[hep-lat/0405028](#)].
- R. Frezzotti *Nucl. Phys. Proc. Suppl.* **140** (2005) 134–140, [[hep-lat/0409138](#)].
- A. Shindler *PoS LAT2005* (2006) 014, [[hep-lat/0511002](#)].
- XLF** Collaboration, K. Jansen, M. Papinutto, A. Shindler, C. Urbach, and I. Wetzorke *JHEP* **09** (2005) 071, [[hep-lat/0507010](#)].
- CP-PACS and JLQCD** Collaboration, A. Ukawa *Nucl. Phys. Proc. Suppl.* **106** (2002) 195–196.
- M. Luscher *Comput. Phys. Commun.* **165** (2005) 199–220, [[hep-lat/0409106](#)].
- C. Urbach, K. Jansen, A. Shindler, and U. Wenger *Comput. Phys. Commun.* **174** (2006) 87–98, [[hep-lat/0506011](#)].
- F. Farchioni *et al.* *Eur. Phys. J.* **C39** (2005) 421–433, [[hep-lat/0406039](#)].
- F. Farchioni *et al.* *Phys. Lett.* **B624** (2005) 324–333, [[hep-lat/0506025](#)].
- F. Farchioni *et al.* *Eur. Phys. J.* **C42** (2005) 73–87, [[hep-lat/0410031](#)].
- S. R. Sharpe and J. Singleton, R. *Phys. Rev.* **D58** (1998) 074501, [[hep-lat/9804028](#)].
- G. Munster *JHEP* **09** (2004) 035, [[hep-lat/0407006](#)].
- F. Farchioni *et al.* *PoS LAT2005* (2006) 072, [[hep-lat/0509131](#)].
- P. Weisz *Nucl. Phys.* **B212** (1983) 1.
- R. Sommer *Nucl. Phys.* **B411** (1994) 839–854, [[hep-lat/9310022](#)].
- G. Colangelo, S. Durr, and C. Haefeli *Nucl. Phys.* **B721** (2005) 136–174, [[hep-lat/0503014](#)].
- ETM** Collaboration *in preparation* (2006).
- G. Colangelo and S. Durr *Eur. Phys. J.* **C33** (2004) 543–553, [[hep-lat/0311023](#)].
- ETM** Collaboration, K. Jansen and C. Urbach [hep-lat/0610015](#).
- P. A. Boyle *et al.* *J. Phys. Conf. Ser.* **16** (2005) 129–139.
- SciDAC** Collaboration, R. G. Edwards and B. Joo *Nucl. Phys. Proc. Suppl.* **140** (2005) 832, [[hep-lat/0409003](#)].
- ApeNEXT** Collaboration, F. Bodin *et al.* *Nucl. Phys. Proc. Suppl.* **140** (2005) 176–182.